Available online at www.sciencedirect.com
ScienceDirect
Physics Letters B 655 (2007) 104–113
PHYSICS LETTERS B
www.elsevier.com/locate/physletb

Energy dependence of $\pi^{\pm}$, p and $\bar{p}$ transverse momentum spectra for Au + Au collisions at $\sqrt{s_{\mathrm{NN}}} = 62.4$ and 200 GeV

STAR Collaboration

B.I. Abelev [i], M.M. Aggarwal [ad], Z. Ahammed [as], B.D. Anderson [t], D. Arkhipkin [m], G.S. Averichev [l], Y. Bai [ab], J. Balewski [q], O. Barannikova [i], L.S. Barnby [b], S. Baumgart [ax], V.V. Belaga [l], A. Bellingeri-Laurikainen [an], R. Bellwied [av], F. Benedosso [ab], R.R. Betts [i], S. Bharadwaj [ai], A. Bhasin [s], A.K. Bhati [ad], H. Bichsel [au], J. Bielcik [ax], J. Bielcikova [ax], A. Billmeier [av], L.C. Bland [c], S.-L. Blyth [v], M. Bombara [b], B.E. Bonner [aj], M. Botje [ab], J. Bouchet [an], A.V. Brandin [z], A. Bravar [c], T.P. Burton [b], M. Bystersky [k], R.V. Cadman [a], X.Z. Cai [am], H. Caines [ax], M. Calderón de la Barca Sánchez [f], J. Callner [i], O. Catu [ax], D. Cebra [f], Z. Chajecki [ac], P. Chaloupka [k], S. Chattopadhyay [as], H.F. Chen [al], J.H. Chen [am], J.Y. Chen [aw], J. Cheng [aq], M. Cherney [j], A. Chikanian [ax], H.A. Choi [ah], W. Christie [c], S.U. Chung [c], J.P. Coffin [r], T.M. Cormier [av], M.R. Cosentino [ak], J.G. Cramer [au], H.J. Crawford [e], D. Das [as], S. Dash [o], M. Daugherity [ap], M.M. de Moura [ak], T.G. Dedovich [l], M. DePhillips [c], A.A. Derevschikov [af], L. Didenko [c], T. Dietel [n], P. Djawotho [q], S.M. Dogra [s], X. Dong [v], J.L. Drachenberg [ao], J.E. Draper [f], F. Du [ax], V.B. Dunin [l], J.C. Dunlop [c], M.R. Dutta Mazumdar [as], V. Eckardt [x], W.R. Edwards [v], L.G. Efimov [l], V. Emelianov [z], J. Engelage [e], G. Eppley [aj], B. Erazmus [an], M. Estienne [r], P. Fachini [c], R. Fatemi [w], J. Fedorisin [l], A. Feng [aw], P. Filip [l], E. Finch [ax], V. Fine [c], Y. Fisyak [c], K.S.F. Fornazier [ak], J. Fu [aw], C.A. Gagliardi [ao], L. Gaillard [b], M.S. Ganti [as], E. Garcia-Solis [i], V. Ghazikhanian [g], P. Ghosh [as], Y.G. Gorbunov [j], H. Gos [at], O. Grebenyuk [ab], D. Grosnick [ar], S.M. Guertin [g], K.S.F.F. Guimaraes [ak], N. Gupta [s], B. Haag [f], T.J. Hallman [c], A. Hamed [ao], J.W. Harris [ax], W. He [q], M. Heinz [ax], T.W. Henry [ao], S. Hepplemann [ae], B. Hippolyte [r], A. Hirsch [ag], E. Hjort [v], A.M. Hoffman [w], G.W. Hoffmann [ap], D. Hofman [i], R. Hollis [i], M.J. Horner [v], H.Z. Huang [g], E.W. Hughes [d], T.J. Humanic [ac], G. Igo [g], A. Iordanova [i], P. Jacobs [v], W.W. Jacobs [q], P. Jakl [k], F. Jia [u], H. Jiang [g], P.G. Jones [b], E.G. Judd [e], S. Kabana [an], K. Kang [aq], J. Kapitan [k], M. Kaplan [h], D. Keane [t], A. Kechechyan [l], D. Kettler [au], V.Yu. Khodyrev [af], B.C. Kim [ah], J. Kiryluk [w], A. Kisiel [at], E.M. Kislov [l], S.R. Klein [v], A.G. Knospe [ax], A. Kocoloski [w], D.D. Koetke [ar], T. Kollegger [n], M. Kopytine [t], L. Kotchenda [z], V. Kouchpil [k], K.L. Kowalik [v], M. Kramer [aa], P. Kravtsov [z], V.I. Kravtsov [af], K. Krueger [a], C. Kuhn [r], A.I. Kulikov [l], A. Kumar [ad], P. Kurnadi [g], A.A. Kuznetsov [l], M.A.C. Lamont [ax], J.M. Landgraf [c], S. Lange [n], S. LaPointe [av], F. Laue [c], J. Lauret [c], A. Lebedev [c], R. Lednicky [l], C.-H. Lee [ah], S. Lehocka [l], M.J. LeVine [c], C. Li [al], Q. Li [av], Y. Li [aq], G. Lin [ax], X. Lin [aw], S.J. Lindenbaum [aa], M.A. Lisa [ac], F. Liu [aw], H. Liu [al], J. Liu [aj], L. Liu [aw], T. Ljubicic [c], W.J. Llope [aj], H. Long [g], R.S. Longacre [c], M. Lopez-Noriega [ac], W.A. Love [c], Y. Lu [aw], T. Ludlam [c], D. Lynn [c], G.L. Ma [am], J.G. Ma [g], Y.G. Ma [am], D.P. Mahapatra [o], R. Majka [ax], L.K. Mangotra [s], R. Manweiler [ar], S. Margetis [t], C. Markert [t], L. Martin [an], H.S. Matis [v], Yu.A. Matulenko [af], C.J. McClain [a], T.S. McShane [j], Yu. Melnick [af], A. Meschanin [af], J. Millane [w], M.L. Miller [w], N.G. Minaev [af], S. Mioduszewski [ao],

0370-2693/$ – see front matter
doi:10.1016/j.physletb.2007.06.035

C. Mironov [t], A. Mischke [ab], J. Mitchell [aj], B. Mohanty [v,*], L. Molnar [ag], D.A. Morozov [af], M.G. Munhoz [ak], B.K. Nandi [p], C. Nattrass [ax], T.K. Nayak [as], J.M. Nelson [b], C. Nepali [t], P.K. Netrakanti [ag], V.A. Nikitin [m], L.V. Nogach [af], S.B. Nurushev [af], G. Odyniec [v], A. Ogawa [c], V. Okorokov [z], M. Oldenburg [v], D. Olson [v], M. Pachr [k], S.K. Pal [as], Y. Panebratsev [l], S.Y. Panitkin [c], A.I. Pavlinov [av], T. Pawlak [at], T. Peitzmann [ab], V. Perevoztchikov [c], C. Perkins [e], W. Peryt [at], S.C. Phatak [o], M. Planinic [ay], J. Pluta [at], N. Poljak [ay], N. Porile [ag], A.M. Poskanzer [v], M. Potekhin [c], E. Potrebenikova [l], B.V.K.S. Potukuchi [s], D. Prindle [au], C. Pruneau [av], J. Putschke [v], I.A. Qattan [q], R. Raniwala [ai], S. Raniwala [ai], R.L. Ray [ap], S.V. Razin [l], J. Reinnarth [an], D. Relyea [d], A. Ridiger [z], H.G. Ritter [v], J.B. Roberts [aj], O.V. Rogachevskiy [l], J.L. Romero [f], A. Rose [v], C. Roy [an], L. Ruan [v], M.J. Russcher [ab], R. Sahoo [o], I. Sakrejda [v], T. Sakuma [w], S. Salur [ax], J. Sandweiss [ax], M. Sarsour [ao], I. Savin [m], P.S. Sazhin [l], J. Schambach [ap], R.P. Scharenberg [ag], N. Schmitz [x], J. Seger [j], I. Selyuzhenkov [av], P. Seyboth [x], A. Shabetai [v], E. Shahaliev [l], M. Shao [al], M. Sharma [ad], W.Q. Shen [am], S.S. Shimanskiy [l], E. Sichtermann [v], F. Simon [w], R.N. Singaraju [as], N. Smirnov [ax], R. Snellings [ab], P. Sorensen [c], J. Sowinski [q], J. Speltz [r], H.M. Spinka [a], B. Srivastava [ag], A. Stadnik [l], T.D.S. Stanislaus [ar], R. Stock [n], M. Strikhanov [z], B. Stringfellow [ag], A.A.P. Suaide [ak], M.C. Suarez [i], N.L. Subba [t], M. Sumbera [k], X.M. Sun [v], Z. Sun [u], B. Surrow [w], T.J.M. Symons [v], A. Szanto de Toledo [ak], J. Takahashi [ak], A.H. Tang [c], T. Tarnowsky [ag], J.H. Thomas [v], A.R. Timmins [b], S. Timoshenko [z], M. Tokarev [l], T.A. Trainor [au], S. Trentalange [g], R.E. Tribble [ao], O.D. Tsai [g], J. Ulery [ag], T. Ullrich [c], D.G. Underwood [a], G. Van Buren [c], N. van der Kolk [ab], M. van Leeuwen [v], A.M. Vander Molen [y], R. Varma [p], I.M. Vasilevski [m], A.N. Vasiliev [af], R. Vernet [r], S.E. Vigdor [q], Y.P. Viyogi [o], S. Vokal [l], S.A. Voloshin [av], W.T. Waggoner [j], F. Wang [ag], G. Wang [g], J.S. Wang [u], X.L. Wang [al], Y. Wang [aq], J.W. Watson [t], J.C. Webb [q], G.D. Westfall [y], A. Wetzler [v], C. Whitten Jr. [g], H. Wieman [v], S.W. Wissink [q], R. Witt [ax], J. Wu [al], J. Wu [aw], N. Xu [v], Q.H. Xu [v], Z. Xu [c], P. Yepes [aj], I.-K. Yoo [ah], Q. Yue [aq], V.I. Yurevich [l], W. Zhan [u], H. Zhang [c], W.M. Zhang [t], Y. Zhang [al], Z.P. Zhang [al], Y. Zhao [al], C. Zhong [am], R. Zoulkarneev [m], Y. Zoulkarneeva [m], A.N. Zubarev [l], J.X. Zuo [am]

[a] *Argonne National Laboratory, Argonne, IL 60439, USA*
[b] *University of Birmingham, Birmingham, United Kingdom*
[c] *Brookhaven National Laboratory, Upton, NY 11973, USA*
[d] *California Institute of Technology, Pasadena, CA 91125, USA*
[e] *University of California, Berkeley, CA 94720, USA*
[f] *University of California, Davis, CA 95616, USA*
[g] *University of California, Los Angeles, CA 90095, USA*
[h] *Carnegie Mellon University, Pittsburgh, PA 15213, USA*
[i] *University of Illinois, Chicago, USA*
[j] *Creighton University, Omaha, NE 68178, USA*
[k] *Nuclear Physics Institute AS CR, 250 68 Řež/Prague, Czech Republic*
[l] *Laboratory for High Energy (JINR), Dubna, Russia*
[m] *Particle Physics Laboratory (JINR), Dubna, Russia*
[n] *University of Frankfurt, Frankfurt, Germany*
[o] *Institute of Physics, Bhubaneswar 751005, India*
[p] *Indian Institute of Technology, Mumbai, India*
[q] *Indiana University, Bloomington, IN 47408, USA*
[r] *Institut de Recherches Subatomiques, Strasbourg, France*
[s] *University of Jammu, Jammu 180001, India*
[t] *Kent State University, Kent, OH 44242, USA*
[u] *Institute of Modern Physics, Lanzhou, China*
[v] *Lawrence Berkeley National Laboratory, Berkeley, CA 94720, USA*
[w] *Massachusetts Institute of Technology, Cambridge, MA 02139-4307, USA*
[x] *Max-Planck-Institut für Physik, Munich, Germany*
[y] *Michigan State University, East Lansing, MI 48824, USA*
[z] *Moscow Engineering Physics Institute, Moscow, Russia*
[aa] *City College of New York, New York City, NY 10031, USA*
[ab] *NIKHEF and Utrecht University, Amsterdam, The Netherlands*
[ac] *Ohio State University, Columbus, OH 43210, USA*
[ad] *Panjab University, Chandigarh 160014, India*

[ae] Pennsylvania State University, University Park, PA 16802, USA
[af] Institute of High Energy Physics, Protvino, Russia
[ag] Purdue University, West Lafayette, IN 47907, USA
[ah] Pusan National University, Pusan, Republic of Korea
[ai] University of Rajasthan, Jaipur 302004, India
[aj] Rice University, Houston, TX 77251, USA
[ak] Universidade de São Paulo, São Paulo, Brazil
[al] University of Science & Technology of China, Hefei 230026, China
[am] Shanghai Institute of Applied Physics, Shanghai 201800, China
[an] SUBATECH, Nantes, France
[ao] Texas A&M University, College Station, TX 77843, USA
[ap] University of Texas, Austin, TX 78712, USA
[aq] Tsinghua University, Beijing 100084, China
[ar] Valparaiso University, Valparaiso, IN 46383, USA
[as] Variable Energy Cyclotron Centre, Kolkata 700064, India
[at] Warsaw University of Technology, Warsaw, Poland
[au] University of Washington, Seattle, WA 98195, USA
[av] Wayne State University, Detroit, MI 48201, USA
[aw] Institute of Particle Physics, CCNU (HZNU), Wuhan 430079, China
[ax] Yale University, New Haven, CT 06520, USA
[ay] University of Zagreb, Zagreb HR-10002, Croatia

Received 26 March 2007; accepted 6 June 2007

Available online 21 June 2007

Editor: V. Metag

Abstract

We study the energy dependence of the transverse momentum (p_T) spectra for charged pions, protons and anti-protons for Au + Au collisions at $\sqrt{s_{NN}} = 62.4$ and 200 GeV. Data are presented at mid-rapidity ($|y| < 0.5$) for $0.2 < p_T < 12$ GeV/c. In the intermediate p_T region ($2 < p_T < 6$ GeV/c), the nuclear modification factor is higher at 62.4 GeV than at 200 GeV, while at higher p_T ($p_T > 7$ GeV/c) the modification is similar for both energies. The p/π^+ and $\bar{p}/\pi^-$ ratios for central collisions at $\sqrt{s_{NN}} = 62.4$ GeV peak at $p_T \simeq 2$ GeV/c. In the p_T range where recombination is expected to dominate, the p/π^+ ratios at 62.4 GeV are larger than at 200 GeV, while the $\bar{p}/\pi^-$ ratios are smaller. For $p_T > 2$ GeV/c, the $\bar{p}/\pi^-$ ratios at the two beam energies are independent of p_T and centrality indicating that the dependence of the $\bar{p}/\pi^-$ ratio on p_T does not change between 62.4 and 200 GeV. These findings challenge various models incorporating jet quenching and/or constituent quark coalescence.

Keywords: Particle production; Recombination; Fragmentation; Jet quenching; Nuclear modification factor; Particle ratios

1. Introduction

Experiments at the Relativistic Heavy Ion Collider (RHIC) [1] at Brookhaven National Laboratory have shown that hadron production at high transverse momentum p_T ($p_T > 6$ GeV/c) is suppressed for central Au + Au collisions relative to nucleon–nucleon collisions or peripheral Au + Au collisions [2,3]. This suppression is thought to be related to jet quenching in dense partonic matter [4]. At intermediate p_T ($2 < p_T < 6$ GeV/c), in central collisions, the baryon to meson ratio is higher than in peripheral collisions [5,6]. This feature may be due to hadronization through the recombination of quarks [7].

The energy loss by energetic partons traversing the dense medium formed in high-energy heavy-ion collisions is predicted to be proportional to both the initial gluon density [8] and the lifetime of the dense matter [9]. The energy dependence of the nuclear modification factor (NMF, defined later) significantly constrains parameters in theoretical model calculations. The quantitatively large suppression pattern observed at high p_T, for both light hadrons and those involving heavy quarks [10], has renewed interest in the mechanism of energy loss, namely, the relative contribution of radiative and collisional forms. The dominance of one over the other depends upon p_T and energy [11,12]. Recently, for a given beam energy a universal dependence of high p_T NMF on the number of participating nucleons (N_{part}) was proposed as a signature of radiative mechanisms being the dominant energy loss processes [13]. On the other hand, it was suggested that radiative energy loss will break x_T ($= 2p_T/\sqrt{s_{NN}}$) scaling [14]. Thus, a detailed study of the energy, p_T, and N_{part} dependence of identified hadron production and hadron scaling properties is needed to continue the investigation of energy loss mechanisms.

In this Letter we report the results of such a study performed using identified charged pions, protons, and anti-protons for rapidities $|y| < 0.5$ and $p_T < 12$ GeV/c for Au + Au at $\sqrt{s_{NN}} =$ 62.4 and 200 GeV. The data were taken by the STAR experiment at RHIC [15].

* Corresponding author.
E-mail address: bmohanty@lbl.gov (B. Mohanty).

Identified particle p_T spectra at different beam energies will also enable the study of the effects of the energy dependence of parton energy loss and initial jet production on the produced hadron p_T spectra. At high p_T ($p_T \gtrsim 6$ GeV/c), pions are expected to originate dominantly from quark jets at $\sqrt{s_{NN}} = 62.4$ GeV, while both gluon and quark jets contribute substantially to pion production in the same p_T region at $\sqrt{s_{NN}} = 200$ GeV [16,17]. Therefore, a factor of ~ 3 difference in x_T (for a given p_T) at the two beam energies may allow the study of the difference in energy loss mechanisms for quarks and gluons. This difference in energy loss is due to the non-Abelian feature of color charge dependence of parton energy loss [18,19]. Alternatively, as $\bar{p}$ production is dominantly from gluon jets, the $p(\bar{p})/\pi$ ratios are sensitive to quark and gluon jet production in heavy-ion collisions [20,21]. Baryon production relative to meson production is also sensitive to baryon transport and energy densities. The energy dependence of the baryon-to-meson ratio will address the specific prediction of the quark coalescence models of a higher baryon-to-meson ratio at $\sqrt{s_{NN}} = 62.4$ GeV compared to 200 GeV in the intermediate p_T range [22].

2. Experiment and analysis

The data presented here were taken at RHIC in 2004 using STAR's [15] Time Projection Chamber (TPC) [23] and a prototype Time-Of-Flight (TOF) [24] detector. The TPC magnetic field was 0.5 Tesla. Using a minimally biased trigger (MB), 7.4×10^6 and 1.4×10^7 Au + Au events at $\sqrt{s_{NN}} = 62.4$ and 200 GeV, respectively, were analyzed. 1.5×10^7 200 GeV Au + Au events from a central trigger were also analyzed, which corresponds to the top 12% of the total cross section [21]. The identified particle spectra for Au + Au collisions at 200 GeV are presented in Ref. [21]. Centrality selection at 62.4 GeV utilized the uncorrected charged particle multiplicity for pseudorapidities $|\eta| < 0.5$, measured by the TPC [21,25]. Ionization energy loss of charged particles in the TPC was used to identify $\pi^{\pm}$, p and $\bar{p}$ within $|\eta| < 0.5$ and full azimuth, for $p_T \leqslant 1.1$ GeV/c and $2.5 \leqslant p_T \leqslant 12$ GeV/c. Detailed descriptions of TPC particle identification techniques for the low p_T range ($0.2 \leqslant p_T \leqslant 2.5$ GeV/c) can be found in Ref. [26]. For $p_T \geqslant 2.5$ GeV/c, the relativistic rise of ionization energy loss was used to identify the $\pi^{\pm}$, p and $\bar{p}$ [21,27]. The TOF data allowed pion and proton identification up to $p_T \sim 3$ GeV/c for $-1 < \eta < 0$ and $\Delta\Phi \leqslant \pi/30$ radians [21,28].

Identified hadron acceptance and tracking efficiency were studied through Monte Carlo GEANT simulations [26,28,29]. At high p_T ($p_T \geqslant 2.5$ GeV/c) the efficiencies range from 73% to 87% and are nearly independent of p_T, but have a weak centrality dependence. Weak-decay feed-down (e.g., $K^0_S \to \pi^+\pi^-$) contributions to the pion spectra were calculated using measured K^0_S and Λ yields [6] and a GEANT simulation. The feed-down contributions to the pion spectra were found to be $\sim 12\%$ at $p_T = 0.35$ GeV/c and decreasing to $\sim 5\%$ for $p_T \geqslant 1$ GeV/c. The final pion spectra are presented after subtracting these contributions. The inclusive p and $\bar{p}$ yields are presented without hyperon feed-down corrections to reflect total baryon production. The corrections range from $< 20\%$ for $p + p$ and $d +$ Au data [26,28,29] rising to $\sim 40\%$ for central Au + Au up to intermediate p_T, and are estimated to be less than 20% at high p_T [21].

Systematic errors for the TPC measurements were particle type and p_T dependent. They include: uncertainties in efficiency ($\sim 8\%$); dE/dx position and width (10–20%); background from decay feed-down, ghost tracks and PID contamination at high p_T (8–14%); momentum distortion due to charge build-up in the TPC volume (0–10%); the distortion of the measured spectra due to momentum resolution (0–5%). The systematic errors are added in quadrature. Systematic errors for the TOF data for $\pi^{\pm}$, p and $\bar{p}$ spectra are similar at both energies and are about 8% [28,30]. The total systematic errors for $\pi^{\pm}$ yields at both energies are estimated to be $\lesssim$15%, and those for p and $\bar{p}$ are $\lesssim 25\%$ over the entire p_T range studied [16].

3. Transverse momentum distribution

Fig. 1 shows $\pi^{\pm}$, p and $\bar{p}$ yields for Au + Au at 62.4 GeV for $0.2 < p_T < 12$ GeV/c and various collision centralities. The hadron spectra at high p_T ($p_T > 6$ GeV/c) for $\sqrt{s_{NN}} = 62.4$ GeV are steeper than the corresponding spectra for $\sqrt{s_{NN}} = 200$ GeV; comparisons of central collision spectra at both energies are shown in Fig. 1. This steepness mostly reflects the difference in initial jet production at the two collision energies. For high-energy $p + p$ and $d +$ Au collisions, particle production at midrapidity is found to follow m_T ($= \sqrt{p_T^2 + \text{mass}^2}$) scaling [16,17]. Such scaling implies that initial parton distributions dominate the particle production process [31]. The possibility of m_T-scaling in heavy-ion collisions has been discussed in Ref. [31]. However, such m_T-scaling is not observed in the data for $\sqrt{s_{NN}} = 62.4$ and 200 GeV Au + Au. This will be evident from $p(\bar{p})/\pi$ ratios presented later. The absence of m_T-scaling may reflect a modification of the initial distributions through both partonic and hadronic final state interactions at RHIC energies.

At $\sqrt{s_{NN}} = 62.4$ GeV, $\pi^-/\pi^+ = 1.01 \pm 0.02$ (stat), independent of p_T within experimental uncertainties (inset of Fig. 1) and collision centrality (not shown). Similar features were observed at 200 GeV [21]. The $\bar{p}/p$ ratios show a slight decrease with p_T (inset of Fig. 1) and are independent of centrality. The decreasing trend is more pronounced at 62.4 GeV [21]. For $p_T < 3$ GeV/c, $\bar{p}/p = 0.44 \pm 0.01$ and 0.77 ± 0.02 at $\sqrt{s_{NN}} = 62.4$ and 200 GeV, respectively. For $p_T > 6$ GeV/c, $\bar{p}/p = 0.29 \pm 0.02$ and 0.70 ± 0.05 at $\sqrt{s_{NN}} = 62.4$ and 200 GeV, respectively.

4. Nuclear modification factor

The nuclear modification factor is defined relative to peripheral collisions (R_{CP}) or relative to nucleon–nucleon collisions (R_{AA}) [2]:

$$R_{CP}(p_T) = \frac{[d^2N/p_T\,dy\,dp_T/\langle N_{bin}\rangle]^{\text{central}}}{[d^2N/p_T\,dy\,dp_T/\langle N_{bin}\rangle]^{\text{peripheral}}},$$

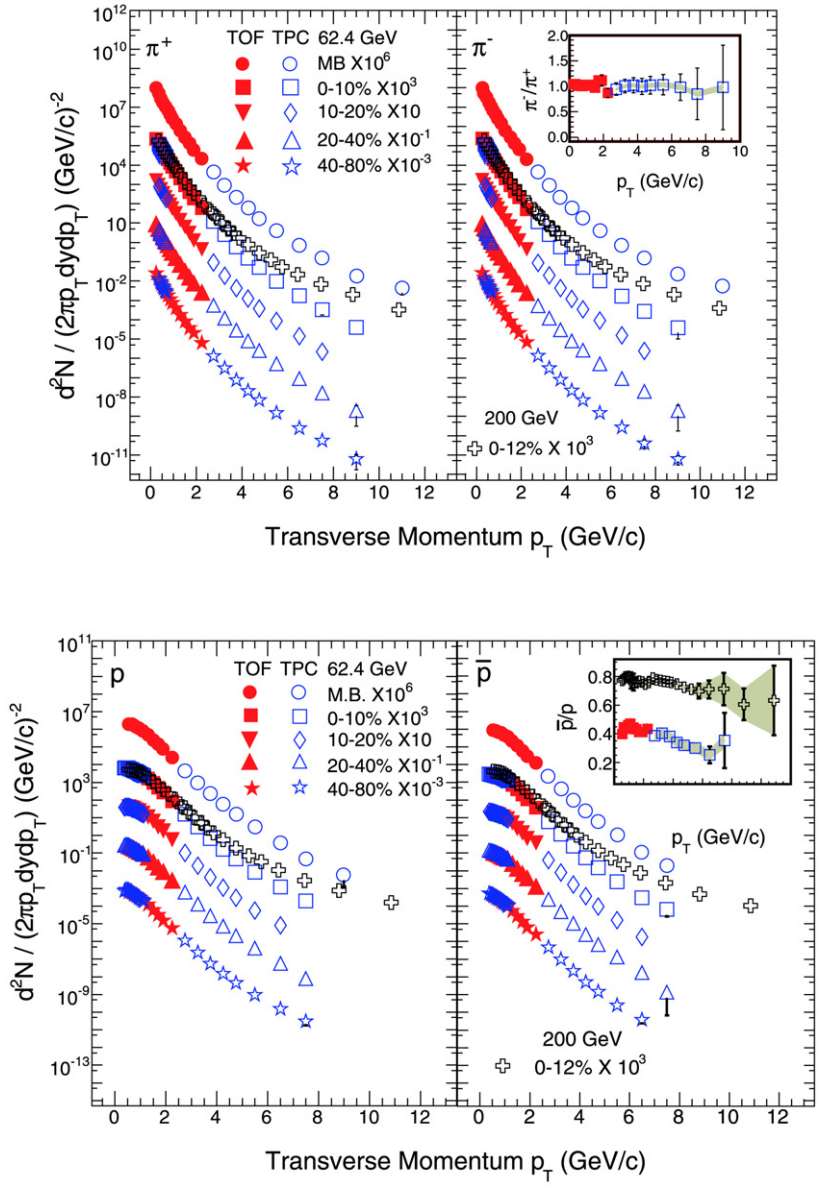

Fig. 1. Midrapidity ($|y| < 0.5$) transverse momentum spectra for $\pi^{\pm}$, p and $\bar{p}$ for various event centrality classes for Au + Au at $\sqrt{s_{\rm NN}} = 62.4$ GeV. Also shown to study the energy dependence are the central 0–12% $\pi^{\pm}$, p and $\bar{p}$ spectra for Au + Au at $\sqrt{s_{\rm NN}} = 200$ GeV. The insets show π^-/π^+ at $\sqrt{s_{\rm NN}} = 62.4$ GeV and $\bar{p}/p$ at $\sqrt{s_{\rm NN}} = 62.4$ (0–10%) and 200 GeV (0–12%). The errors shown are statistical, and the shaded bands reflect the systematic errors.

where $\langle N_{\rm bin}\rangle$ is the average number of binary nucleon–nucleon collisions per event, and

$$R_{\rm AA}(p_{\rm T}) = \frac{d^2N_{\rm AA}/dy\,dp_{\rm T}/\langle N_{\rm bin}\rangle}{d^2\sigma_{pp}/dy\,dp_{\rm T}/\sigma_{pp}^{\rm inel}}.$$

The $\sigma_{\rm pp}^{\rm inel}$ are taken to be 36 mb and 42 mb for $\sqrt{s_{\rm NN}} = 62.4$ GeV and 200 GeV, respectively [32]. The $d^2\sigma_{\rm pp}/dy\,dp_{\rm T}$ at 200 GeV are from STAR measurements [16]; for 62.4 GeV we use a parametrization of ISR data [33] in which the π invariant yield for $p + p$ at $\sqrt{s_{\rm NN}} = 62.4$ GeV is parameterized as $E\,d^3\sigma_{\rm pp\to\pi X}/d^3p = A(e^{a\cdot p_{\rm T}^2 + b\cdot p_{\rm T}} + p_{\rm T}/p_0)^{-n}$, with $A = 265.1$ mb GeV$^{-2}\,c^3$, $a = -0.0129$ GeV$^{-2}\,c^2$, $b = 0.04975$ GeV$^{-1}\,c$, $p_0 = 2.639$ GeV/c, and $n = 17.95$. The uncertainty in yields associated with this parametrization is $\sim 25\%$.

Fig. 2 (upper panels) shows the $p_{\rm T}$, centrality and $\sqrt{s_{\rm NN}}$ dependence of $R_{\rm CP}$ for $\pi^+ + \pi^-$ and $p + \bar{p}$ for Au + Au. The bottom panels show the $\pi^+ + \pi^-$ $R_{\rm AA}$ for the 0–10% and 0–12% centralities at $\sqrt{s_{\rm NN}} = 62.4$ and 200 GeV, respectively. For a given energy there is a distinct difference in the $p_{\rm T}$ dependence between the $R_{\rm CP}$ for $\pi^+ + \pi^-$ and the $R_{\rm CP}$ for $p + \bar{p}$ at intermediate $p_{\rm T}$. The $R_{\rm CP}$ for $p + \bar{p}$ has a steeper fall with $p_{\rm T}$ compared to $\pi^+ + \pi^-$. At high $p_{\rm T}$ the $R_{\rm CP}$ values are similar for baryons and mesons at both energies. The relevance of these measurements for understanding the energy loss of quarks, gluons and their interaction with the medium will be discussed together with the p/π^+ and $\bar{p}/\pi^-$ ratios in the next

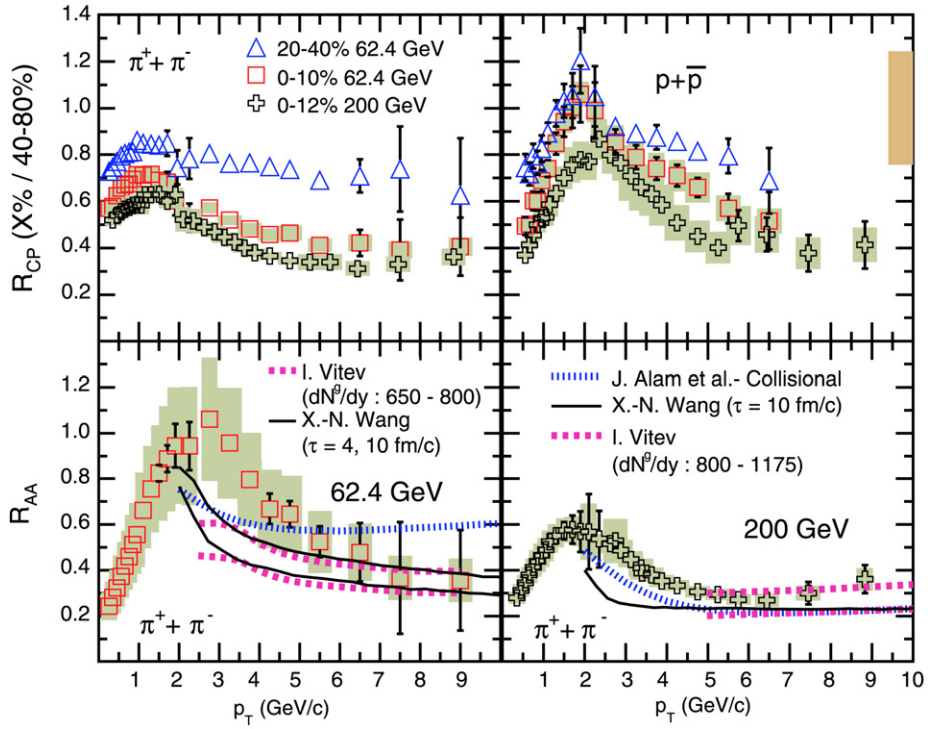

Fig. 2. Upper panels: Centrality and p_T dependence of R_{CP} for $\pi^+ + \pi^-$ and $p + \bar{p}$ for Au + Au at $\sqrt{s_{NN}} = 62.4$ GeV. For studying the energy dependence, the corresponding R_{CP} for central 0–12% Au + Au at $\sqrt{s_{NN}} = 200$ GeV are shown. Lower panels: R_{AA} for $\pi^+ + \pi^-$ at 62.4 GeV (0–10%) and 200 GeV (0–12%) compared to three model predictions [8,9,11] (see text for details). A 25% uncertainty is associated with $d^2\sigma_{pp}/dy\,dp_T$ at 62.4 GeV. The error bars are statistical; the shaded bands are the systematic errors. The systematic errors for the 20–40% centrality data are of similar order as those shown for the 0–10% data. The shaded band around $R_{CP} = 1$ at $p_T = 10$ GeV/c in the top right panel reflects the uncertainty in $\langle N_{bin} \rangle$ calculation for 0–10% collision centrality.

section. When compared as a function of centrality, a dependence is observed for R_{CP} for both $\pi^+ + \pi^-$ and $p + \bar{p}$ at $\sqrt{s_{NN}} = 62.4$ GeV. It is found to be stronger for $\pi^+ + \pi^-$. A similar decrease in R_{CP} values with increasing collision centrality was observed at $\sqrt{s_{NN}} = 200$ GeV [21]. The R_{CP} values at $\sqrt{s_{NN}} = 62.4$ GeV are higher than at $\sqrt{s_{NN}} = 200$ GeV for $p_T < 7$ GeV/c; beyond this p_T they approach each other; this feature may be due to the interplay of initial jet production and the gluon density. For a smaller initial gluon density at the lower energy, the R_{CP} values at the two beam energies may approach each other at high p_T due to a steeper initial jet spectrum at 62.4 GeV [18].

The charged pion R_{AA} (left bottom panel of Fig. 2) for $3.0 < p_T < 8.0$ GeV/c at $\sqrt{s_{NN}} = 62.4$ GeV decreases with p_T and approaches ~ 0.35 at $p_T = 8$ GeV/c. In contrast the R_{AA} values at $\sqrt{s_{NN}} = 200$ GeV are fairly constant for $p_T > 4.0$ GeV/c (bottom right panel). The difference in the p_T dependence of R_{AA} at the two beam energies is influenced by the energy dependence of the following: the shape of the initial jet spectrum, the parton energy loss, and the relative contributions of quark and gluon jets. The steeper fall in R_{AA} with p_T at 62.4 GeV may be due to the steeper initial jet spectrum. The constant value of R_{AA} at high p_T for 200 GeV indicates that the effect due to the shape of the jet spectrum seems to be compensated by the parton energy loss. In addition, as quarks are expected to lose less energy than gluons in the medium [18,19], a higher contribution of quark jets at 62.4 GeV compared to 200 GeV for the same p_T ($x_T^{62.4}/x_T^{200} \sim 3$) may also cause a difference in the energy dependence of R_{AA} versus p_T. The differences in the high-p_T dependence of R_{AA} at the two collision energies rules out x_T-scaling for Au + Au [34][1] in contrast to the observations for $p + p$ [16]. This is expected, as various additional non-perturbative and perturbative processes for particle production in heavy-ion collisions have distinct p_T and $\sqrt{s_{NN}}$ dependencies.

In Fig. 2 the charged pion R_{AA} are compared to model predictions at both energies to study their dependence on the initial gluon density, the lifetime of dense matter and the mechanism of energy loss. The predictions shown do not agree with the data in the region $2 < p_T < 4$ GeV/c, indicating that non-perturbative processes may dominate hadron production in this p_T range. The dashed curves are from a set of calculations which are sensitive to the choice of initial gluon density [8,35]. Comparison at high p_T shows that the initial gluon densities (dN^g/dy) are about 650–800 and 800–1175 from these calculations for Au + Au at $\sqrt{s_{NN}} = 62.4$ and 200 GeV, respectively. The lower dashed curves are for higher gluon density. In addition, theoretical studies also suggest that for a given initial density, the $R_{AA}(p_T)$ values are sensitive to the life-

[1] Earlier it was reported that neutral pions show x_T-scaling in the region $0.03 < x_T < 0.06$ for $\sqrt{s_{NN}} = 130$ and 200 GeV with an effective scaling power of 6.41 ± 0.49 [34]. We did a similar study for the charged pions at $\sqrt{s_{NN}} = 62.4$ and 200 GeV and found x_T-scaling in a different region $0.06 < x_T < 0.11$ with a higher effective scaling power of 7.4 ± 0.2 for central Au + Au.

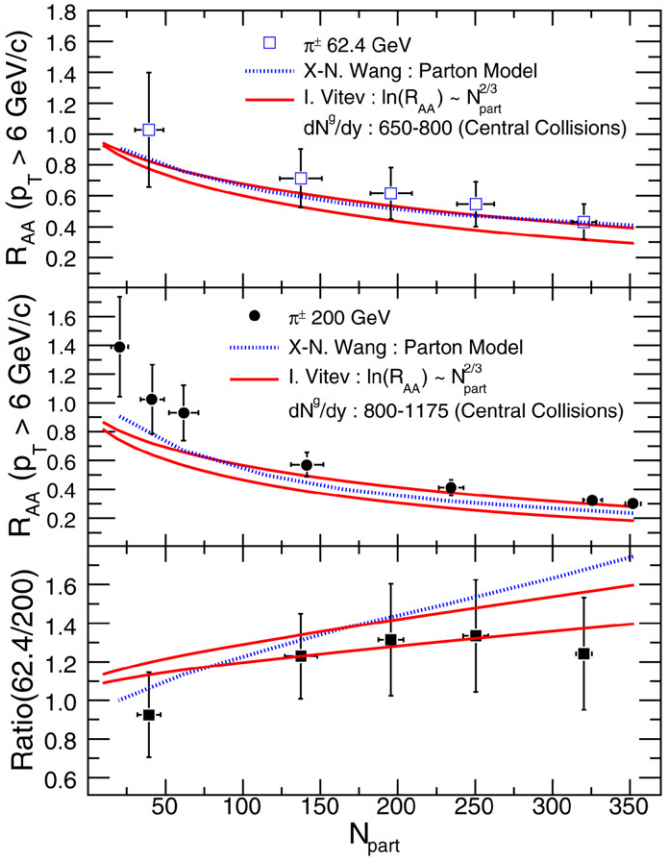

Fig. 3. $R_{AA}(p_T > 6\ \mathrm{GeV}/c)$ versus N_{part} for charged pions for Au + Au at 62.4 GeV and 200 GeV, and their ratio. The error bars are statistical and systematic errors added in quadrature. The solid curves are results of calculations with radiative energy loss for two different initial gluon densities in central collisions at both energies and then following the dependence of $\ln(R_{AA}) \propto N_{part}^{2/3}$ [13]. The dotted curves are theoretical calculations based on a parton model (see text for details) [36].

time (τ) of dense matter formed in heavy-ion collisions [9]. The solid curves are predictions from Ref. [9] at $\sqrt{s_{NN}} = 62.4$ and 200 GeV with $\tau = 10$ fm/c (i.e., larger than the typical system size of ~ 6–7 fm). For 62.4 GeV, also shown is a prediction with $\tau = 4$ fm/c (upper solid line). The comparison at high p_T shows that, for this model, the lifetime of the dense matter formed in Au + Au collisions at $\sqrt{s_{NN}} = 62.4$ and 200 GeV is comparable or larger than the system size. Further insight to the mechanism of energy loss is obtained by comparing the data to theoretical predictions (dotted curves) of R_{AA} from models that consider only collisional energy loss [11]. For $\sqrt{s_{NN}} = 200$ GeV, the model predictions of R_{AA} at high p_T are close to the measured values and similar to corresponding R_{AA} values from models based on only a radiative mechanism for parton energy loss. However, collisional energy loss model overpredicts the experimental R_{AA} values at $\sqrt{s_{NN}} = 62.4$ GeV and shows a stronger dependence on beam energy compared to models based on the radiative process of parton energy loss.

The centrality dependence of R_{AA} at high p_T may provide information on the path length dependence of parton energy loss in heavy-ion collisions. Fig. 3 shows R_{AA} $(p_T > 6\ \mathrm{GeV}/c)$ as a function of N_{part} for $\pi^+ + \pi^-$ for Au + Au at 62.4 and 200 GeV. The R_{AA} values decrease with N_{part} at both energies. The data are compared to results of two types of model calculations. The solid curves are from a model that uses a radiative energy loss mechanism for partons propagating through the medium formed in heavy-ion collisions [13]. The model assumes the parton production cross section to be a power law type and a parton energy loss that depends on the initial gluon density, the path length traveled by the parton, and the transverse area of the region of the collision. Such a model predicts the centrality dependence of high p_T R_{AA} at a given beam energy to be of the form $\ln(R_{AA}) \sim N_{part}^{2/3}$ [13]. The calculations are done for a set of two different gluon densities at both energies. The data follow the predicted dependence at both energies down to low values of N_{part}.

The dotted curves in Fig. 3 are results from a pQCD based parton model in which parton interactions with the medium formed in heavy-ion collisions are reflected through the modification of its fragmentation function [36]. The partons in the medium lose energy by induced gluon radiation. In such models, the parton energy loss depends upon the local gluon density and the total distance of parton propagation [36]. These predictions are in reasonable agreement with the data for most of the centrality classes studied.

The difference between the two models becomes clearer when we compare the ratio of R_{AA} $(p_T > 6\ \mathrm{GeV}/c)$ values at 62.4 and 200 GeV with the ratios from data. This is shown in the bottom panel of Fig. 3. For the data, the R_{AA} versus N_{part} at 200 GeV is first parametrized by a polynomial function and then the ratios of R_{AA} (62.4)/R_{AA} (200) are calculated. The pQCD based parton model overpredicts the measurements for the most central collisions. For the most peripheral collisions measured, the model calculations from Ref. [13] overpredict the data. It will be interesting to compare the R_{AA} versus N_{part} for models with collisional energy loss and see if they provide further constraint on mechanism of energy loss of partons in heavy-ion collisions.

5. Baryon-to-meson and anti-baryon-to-baryon ratios

Fig. 4 shows the p/π^+ and $\bar{p}/\pi^-$ ratios versus p_T for Au + Au 0–10% and 0–12% (upper panels), and 40–80% (lower panels) centralities at $\sqrt{s_{NN}} = 62.4$ GeV and 200 GeV, together with theoretical predictions to be discussed.

The fact that for central collisions the p/π^+ and $\bar{p}/\pi^-$ ratios are close to unity in the intermediate p_T region at 200 GeV has been attributed to either quark coalescence [7,22] or novel baryon transport dynamics based on topological gluon field configurations [37]. The quark coalescence models predict a specific energy dependence for p/π^+, being higher at $\sqrt{s_{NN}} =$ 62.4 GeV than at 200 GeV in the intermediate p_T region; the energy dependence is reversed for $\bar{p}/\pi^-$ [22]. On the other hand, the baryon junction model predicts a decrease in the ratio at intermediate p_T with decreasing collision centrality at a given $\sqrt{s_{NN}}$ [37].

As Fig. 4 shows, at a given p_T the p/π^+ ratio for Au + Au at 62.4 GeV is larger than the value at 200 GeV in the intermediate p_T range, whereas for $\bar{p}/\pi^-$ the reverse occurs. This specific

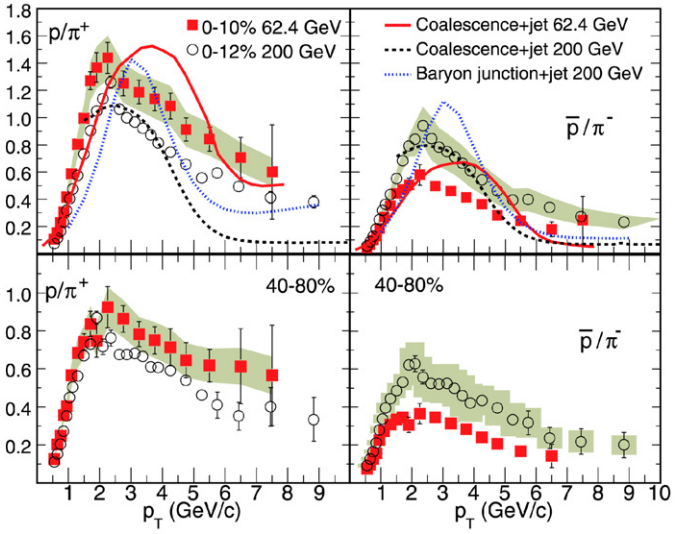

Fig. 4. p/π^+ and $\bar{p}/\pi^-$ ratios versus p_T at $\sqrt{s_{NN}} = 62.4$ and 200 GeV for central (upper panels) and peripheral (lower panels) collisions. For clarity of presentation, the systematic errors (shaded bands) are shown for only one of the beam energy for a given ratio. They are of similar magnitude at the other beam energy. The curves are model results [22,37,38] and are discussed in the text.

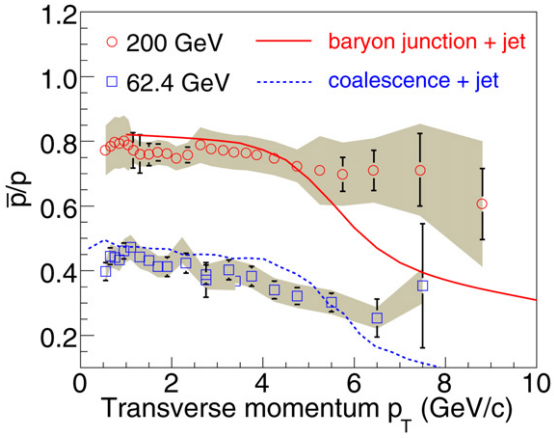

Fig. 5. The $\bar{p}/p$ ratios versus p_T at $\sqrt{s_{NN}} = 62.4$ (0–10%) and 200 GeV (0–12%). The errors shown are statistical, and the shaded bands reflect the systematic errors. Model predictions are shown as solid and dashed curves for 200 GeV [37] and 62.4 GeV [22] central Au + Au, respectively.

energy dependence of the baryon-to-meson ratio as a function of p_T is consistent with the general expectation from quark coalescence models [22]. Our results also show that the baryon-to-meson ratios, here p/π^+, for the region $1.5 < p_T < 6$ GeV/c are higher than in $p + p$ and $d + $ Au [16]. This enhancement increases with centrality for both beam energies.

The ratios for the 0–10% and 0–12% centrality data (upper panels of Fig. 4) are compared to predictions from models based on quark coalescence and a jet fragmentation mechanism for particle production at 62.4 GeV [22] and 200 GeV [38], and baryon junction and jet fragmentation at 200 GeV [37]. For the intermediate p_T region there is a lack of quantitative agreement between model results and data. The recombination models predict a shift in the peak position of the ratios to higher p_T at the 62.4 GeV, which is not observed. The $\bar{p}/\pi^-$ ratios for the two energies do not cross-over as predicted by the models. The baryon junction model predictions are not in quantitative agreement with our 200 GeV data.

At higher p_T the p/π^+ and $\bar{p}/\pi^-$ ratios are nearly independent of centrality at both 62.4 and 200 GeV. This observation, taken together with a constant R_{CP} beyond $p_T > 6$ GeV/c, may reflect the dominance of particle production from the fragmentation mechanism. Also, at high p_T ($p_T > 6$ GeV/c) we observed a similar $\bar{p}/\pi^-$ ratio in central Au + Au and d + Au at 200 GeV [16,21] and a similar R_{CP} for $p + \bar{p}$ and $\pi^+ + \pi^-$ for Au + Au (see previous section). These observations appear to be inconsistent with the naive expectations from the color charge dependence of the parton energy loss [18,19]. The difference in quark and gluon energy loss would have led to a lower $\bar{p}/\pi^-$ ratio for Au + Au at high p_T than that for d + Au collisions and a lower R_{CP} for $p + \bar{p}$ compared to $\pi^+ + \pi^-$. Recent theoretical calculations suggest that a much larger net quark to gluon jet conversion rate in the QGP medium is needed than given by the lowest order QCD calculations to explain the high p_T particle ratios [20].

As one can see in Fig. 4, the jet fragmentation prediction is reasonable at high p_T for the p/π^+ ratios at 62.4 GeV. However these calculations predict a much lower value for the ratio at 200 GeV. The failure of these model calculations at high p_T is further noticeable when we compare them to the measured $\bar{p}/p$ ratios at both energies. Fig. 5 shows the $\bar{p}/p$ ratios versus p_T at 62.4 and 200 GeV. The data are compared to a model result in which baryons and anti-baryons are produced through baryon junctions and jet fragmentation at 200 GeV [37] and through coalescence and jet fragmentation processes at 62.4 GeV [22]. Both the models overpredict the data at lower p_T ($p_T < 5$ GeV/c). For $p_T > 6$ GeV/c, where fragmentation is the dominant mechanism of particle production in the models, they underpredict the measured $\bar{p}/p$ ratios at the two beam energies. The model calculations do not use the recent fragmentation functions for $p + \bar{p}$ as supported by the RHIC data from $p + p$ and $d + $ Au collisions at 200 GeV [16].

To further investigate the energy dependence of baryon-to-meson ratios, we present the ratio of $\bar{p}/\pi^-$ between 62.4 GeV and 200 GeV and the ratio of p/π^+ between 62.4 GeV and 200 GeV. Fig. 6 shows that this double ratio of $\bar{p}/\pi^-$ is independent of p_T with a value around 0.6 for $p_T > 2$ GeV/c, while the double ratio of p/π^+ is around 1.2 for $p_T \simeq 2 - 5$ GeV/c and increases with p_T, possibly due to different valence quark contributions at the two energies.

Baryon and meson production at high p_T and the relative contributions from quark and gluon jets have been discussed in Refs. [16,21]. The new observations presented in this Letter necessitate further understanding of the role of gluons, quarks and their energy loss mechanisms. Gluon jets tend to produce more baryons than quark jets, whereas quark jets contributes substantially to pion production. This feature is supported by a much lower $\bar{p}/\pi^-$ ratio at high p_T compared to the p/π^+ ratio for low-energy $p + p$ and $p + $A collisions [16]. The double ratios in Fig. 6 are consistent with this picture as the $\bar{p}/\pi^-$ ratio is lower at 62 GeV than at 200 GeV. Due to their larger coupling

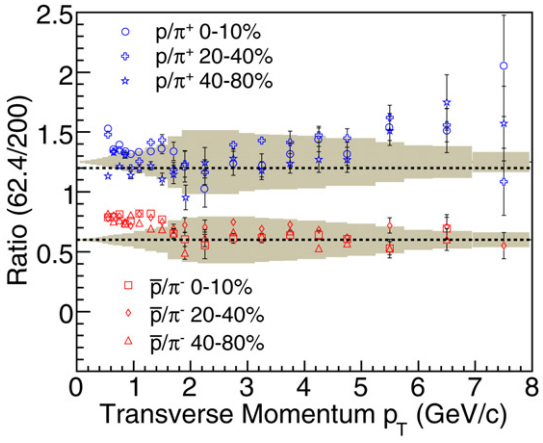

Fig. 6. The ratios p/π^+ at $\sqrt{s_{\rm NN}} = 62.4$ GeV and 200 GeV and $\bar{p}/\pi^-$ at $\sqrt{s_{\rm NN}} = 62.4$ GeV and 200 GeV as functions of $p_{\rm T}$ for various collision centrality classes. The error bars are statistical and shaded bands are the systematic errors.

gluons should lose more energy in the dense medium formed in heavy-ion collisions than quarks [18,19]. This would lead to a lower $\bar{p}/\pi^-$ ratio for central Au + Au relative to peripheral Au + Au at both beam energies. This is not observed for the data reported here. A larger value of the p/π^+ ratio at 62 GeV than at 200 GeV is observed. This may be due to greater valence quark contribution at the lower beam energy. However, the p/π^+ double ratio shows no centrality dependence. This is not expected if valence quarks contribute significantly more at lower energy and lose energy in the dense medium formed for central Au + Au.

At intermediate $p_{\rm T}$, the features of the double ratios are not expected from the coalescence model; as seen in Fig. 4 the quark coalescence models will lead to more prominent baryon enhancement at 62 GeV than at 200 GeV. It is, however, surprising that the scaling is independent of centrality and extends to high $p_{\rm T}$ when baryons are more enhanced at intermediate $p_{\rm T}$.

6. Summary

We have presented a study of the energy dependence of $\pi^{\pm}$, p and $\bar{p}$ production for Au + Au at $\sqrt{s_{\rm NN}} = 62.4$ and 200 GeV. The $p_{\rm T}$ spectra are measured around midrapidity ($|y| < 0.5$) over the range $0.2 < p_{\rm T} < 12$ GeV/c. These measurements provide new experimental data for investigating the production of quarks, gluons and their interactions with the medium formed in heavy-ion collisions and the interplay between coalescence of thermal partons and jet fragmentation.

The $p_{\rm T}$ dependence of $R_{\rm CP}$ for charged pions and for protons and anti-protons is different at both energies. However, at higher $p_{\rm T}$ the values of $R_{\rm CP}$ for baryons and mesons at both energies are similar. The comparison of $R_{\rm AA}$ versus $p_{\rm T}$ to model predictions provides important information on quantities like initial gluon density and lifetime of dense matter.

The p/π^+ ratios for Au + Au at $\sqrt{s_{\rm NN}} = 62.4$ GeV are higher than the corresponding values at $\sqrt{s_{\rm NN}} = 200$ GeV in the intermediate $p_{\rm T}$ range, but the $\bar{p}/\pi^-$ ratios are smaller. There is serious quantitative disagreement between data and the available theoretical models. We observe a scaling of the $\bar{p}/\pi^-$ ratios between corresponding centralities for the two beam energies at $p_{\rm T} > 2$ GeV/c despite the strong centrality and $p_{\rm T}$ dependence of these ratios.

Acknowledgements

We thank J. Alam, V. Greco, C.M. Ko, I. Vitev and X.-N. Wang for providing the theoretical results for comparison with the data. We thank the RHIC Operations Group and RCF at BNL, and the NERSC Center at LBNL for their support. This work was supported in part by the Offices of NP and HEP within the US DOE Office of Science; the US NSF; the BMBF of Germany; CNRS/IN2P3, RA, RPL, and EMN of France; EPSRC of the United Kingdom; FAPESP of Brazil; the Russian Ministry of Science and Technology; the Ministry of Education and the NNSFC of China; IRP and GA of the Czech Republic, FOM of the Netherlands, DAE, DST, and CSIR of the Government of India; Swiss NSF; the Polish State Committee for Scientific Research; SRDA of Slovakia, and the Korea Sci. & Eng. Foundation.

References

[1] BRAHMS Collaboration, I. Arsene, et al., Nucl. Phys. A 757 (2005) 1; PHOBOS Collaboration, B.B. Back, et al., Nucl. Phys. A 757 (2005) 28; STAR Collaboration, J. Adams, et al., Nucl. Phys. A 757 (2005) 102; PHENIX Collaboration, K. Adcox, et al., Nucl. Phys. A 757 (2005) 184.
[2] STAR Collaboration, J. Adams, et al., Phys. Rev. Lett. 91 (2003) 072304; STAR Collaboration, J. Adams, et al., Phys. Rev. Lett. 91 (2003) 172302.
[3] PHENIX Collaboration, S.S. Adler, et al., Phys. Rev. Lett. 91 (2003) 072301.
[4] X.-N. Wang, M. Gyulassy, Phys. Rev. Lett. 68 (1992) 1480; R. Baier, Y.L. Dokshitzer, S. Peigne, D. Schiff, Phys. Lett. B 345 (1995) 277; M. Gyulassy, I. Vitev, X.-N. Wang, B.-W. Zhang, in: R.C. Hwa, X.N. Wang (Eds.), Quark Gluon Plasma 3, World Scientific, Singapore, 2003, p. 123, nucl-th/0302077; P. Levai, G. Papp, G.I. Fai, M. Gyulassy, G.G. Barnafoldi, I. Vitev, Y. Zhang, Nucl. Phys. A 698 (2002) 631.
[5] PHENIX Collaboration, S.S. Adler, et al., Phys. Rev. Lett. 91 (2003) 172301.
[6] STAR Collaboration, J. Adams, et al., Phys. Rev. Lett. 92 (2004) 052302.
[7] V. Greco, C.M. Ko, P. Levai, Phys. Rev. Lett. 90 (2003) 202302; R.J. Fries, B. Muller, C. Nonaka, S.A. Bass, Phys. Rev. Lett. 90 (2003) 202303.
[8] I. Vitev, M. Gyulassy, Phys. Rev. Lett. 89 (2002) 252301.
[9] X.-N. Wang, Phys. Rev. C 70 (2004) 031901(R).
[10] STAR Collaboration, B.I. Abelev, et al., nucl-ex/0607012.
[11] J. Alam, et al., Phys. Rev. D 71 (2005) 094016; J. Alam, et al., hep-ph/0604131.
[12] M.G. Mustafa, Phys. Rev. C 72 (2005) 014905.
[13] I. Vitev, Phys. Lett. B 639 (2006) 38.
[14] S.J. Brodsky, H.J. Pirner, J. Raufeisen, Phys. Lett. B 637 (2006) 58.
[15] K.H. Ackerman, et al., Nucl. Instrum. Methods Phys. Res., Sect. A 499 (2003) 624.
[16] STAR Collaboration, J. Adams, et al., Phys. Lett. B 637 (2006) 161.
[17] STAR Collaboration, B.I. Abelev, et al., nucl-ex/0607033.
[18] X.-N. Wang, Phys. Rev. C 58 (1998) 2321; Q. Wang, X.-N. Wang, Phys. Rev. C 71 (2005) 014903.
[19] S. Wicks, et al., Nucl. Phys. A 784 (2007) 426; N. Armesto, et al., Phys. Rev. D 71 (2005) 054027.
[20] W. Liu, C.M. Ko, B.W. Zhang, nucl-th/0607047.

[21] STAR Collaboration, B.I. Abelev, et al., Phys. Rev. Lett. 97 (2006) 152301.
[22] V. Greco, C.M. Ko, I. Vitev, Phys. Rev. C 71 (2005) 041901(R).
[23] M. Anderson, et al., Nucl. Instrum. Methods A 499 (2003) 659.
[24] B. Bonner, et al., Nucl. Instrum. Methods A 508 (2003) 181;
M. Shao, et al., Nucl. Instrum. Methods A 492 (2002) 344.
[25] STAR Collaboration, J. Adams, et al., Phys. Rev. C 73 (2006) 034906.
[26] STAR Collaboration, J. Adams, et al., Phys. Rev. Lett. 92 (2004) 112301.
[27] M. Shao, et al., Nucl. Instrum. Methods A 558 (2006) 419;
H. Bichsel, Nucl. Instrum. Methods A 562 (2006) 154.
[28] STAR Collaboration, J. Adams, et al., Phys. Lett. B 616 (2005) 8.
[29] STAR Collaboration, C. Adler, et al., Phys. Rev. Lett. 87 (2001) 262302.
[30] L. Ruan, Ph.D. thesis, University of Science and Technology of China, 2004, nucl-ex/0503018.
[31] J. Schaffner-Bielich, D. Kharzeev, L. McLerran, R. Venugopalan, Nucl. Phys. A 705 (2002) 494.
[32] S. Eidelman, et al., Phys. Lett. B 592 (2004) 315.
[33] D. d'Enterria, J. Phys. G 31 (2005) S491.
[34] PHENIX Collaboration, S.S. Adler, et al., Phys. Rev. C 69 (2004) 034910.
[35] I. Vitev, Phys. Lett. B 606 (2005) 303.
[36] X.-N. Wang, Nucl. Phys. A 774 (2006) 215.
[37] I. Vitev, M. Gyulassy, Phys. Rev. C 65 (2002) 041902(R);
I. Vitev, M. Gyulassy, Nucl. Phys. A 715 (2003) 779c.
[38] R.J. Fries, et al., Phys. Rev. C 68 (2003) 044902.